

# Wireless Implants

Rizwan Bashirullah



© PHOTODISC

**I**n vivo wireless biomedical microsystems fueled by the continued scaling of electronic components and the development of new microsensors and micropackaging technologies is rapidly changing the landscape of the electronics and medical industry. These devices can be used for a myriad of monitoring, diagnostic, therapeutic, and interventional applications that range from the well known cardiac pacemakers and defibrillators to emerging applications in visual prosthesis, brain computer interfaces (BCIs), and embedded monitoring of a variety of medical useful variables such as oxygen, glucose, pH level, pressure, and core temperature. This article presents a brief overview of design considerations for implementing wireless power and data interfaces for in vivo biomedical devices. Examples of emerging implantable and ingestible wireless biomedical devices are discussed.

## Parameterization of Hardware Challenges

The requirements imposed on in vivo biomedical devices are application specific, but the framework for hardware implementation shares a common set of constraints in size, power, and functionality. The interplay between these constraints determines the available processing bandwidth for the front-end electronics, the operating time in battery powered implants, and the communication range and bandwidth of the wireless link.

Figure 1 shows an example parameterization of various biomedical technologies in terms of size, power, and functionality. Restricting the overall size of the biomedical

---

Rizwan Bashirullah ([rizwan@tec.ufl.edu](mailto:rizwan@tec.ufl.edu)) is with the Department of Electrical and Computer Engineering, University of Florida, Gainesville FL 32611, USA.

Digital Object Identifier 10.1109/MMM.2010.938579

device can impact the functional specifications, power efficiency, and compute capacity of the entire system. For instance, battery-operated devices with stringent size restrictions ( $<10 \text{ mm}^2$ ) are functionally limited by the size of the battery and hence the available capacity, peak power handling capability and overall lifetime. In addition, the size restrictions also limit the attainable radiation efficiencies of electrically small antennas, thereby affecting the power budget of the communication link. Increased system functionality such as higher sensor resolution, channel count, computational bandwidth, and transmission data rates generally implies higher power dissipation and larger implant size. Thus, from a hardware perspective, design considerations are driven by trade-offs in size, power, and system functionality, wherein highly functional, ultralow-power, and miniature in vivo devices are generally most challenging.

## Wireless Power and Data Links

### Inductive Links

Wireless powering of implantable electronics is commonly achieved via low-frequency inductive links [1], [2], as at low frequency the magnetic fields are well penetrable in biological media [3]. However, because the magnetic field strength over the coil axis falls as a third power of distance, this type of link is suitable only for very small distances. Several studies have been conducted to measure the mutual inductance between two air-coupled coils [4], [5]. Coupling strength is dependent on coil loading, excitation frequency, coaxial alignment, coil separation, coil geometry, and angular alignment. Most of these are subject to variations and typical values for coil-coupling are between 0.01 and 0.2.

Figure 2 shows the basic components of an inductively coupled power and bidirectional data telemetry link using a primary external inductor and a secondary implant inductor. The extracorporeal transmitter typically consists of a class-E amplifier owing to the high-achievable efficiencies ( $>95\%$ ) and ability to induce large voltages (that is, 50–200 V) across the primary coil from a relatively low-voltage power source such as a battery [6]. On the implant side, the induced voltage that appears in the secondary coil is generally passively resonated using a capacitor to boost the voltage and then rectified and regulated to provide a clean supply for the on-chip electronics. Forward data telemetry towards the implant is commonly implemented by modulating the envelope of the power carrier to create detectable changes in the secondary coil. Reverse telemetry or backtelemetry from the implant toward the external unit is generally based on the load modulation technique, also known as “load shift keying” [1], [2], [7], wherein the reflected impedance in the primary coil is modulated by changing the impedance seen by the secondary coil. To minimize radio frequency (RF) heating due to tissue absorption, these inductive links are generally operated below 10 MHz with typical output power ranging from 10–250 mW, and practical achievable data-rates of 1–2 Mb/s [8].

### Low-Power Data Telemetry

The design complexity and power dissipation of telemetry links for in vivo biomedical devices depends on numerous factors, including but not limited to the desired operating range, implant size, location of the implant in the body, data rate, frequency, and regulatory standards. For very-short-range links (that is, 1–10 s of centimeters), low-frequency inductive links provide a

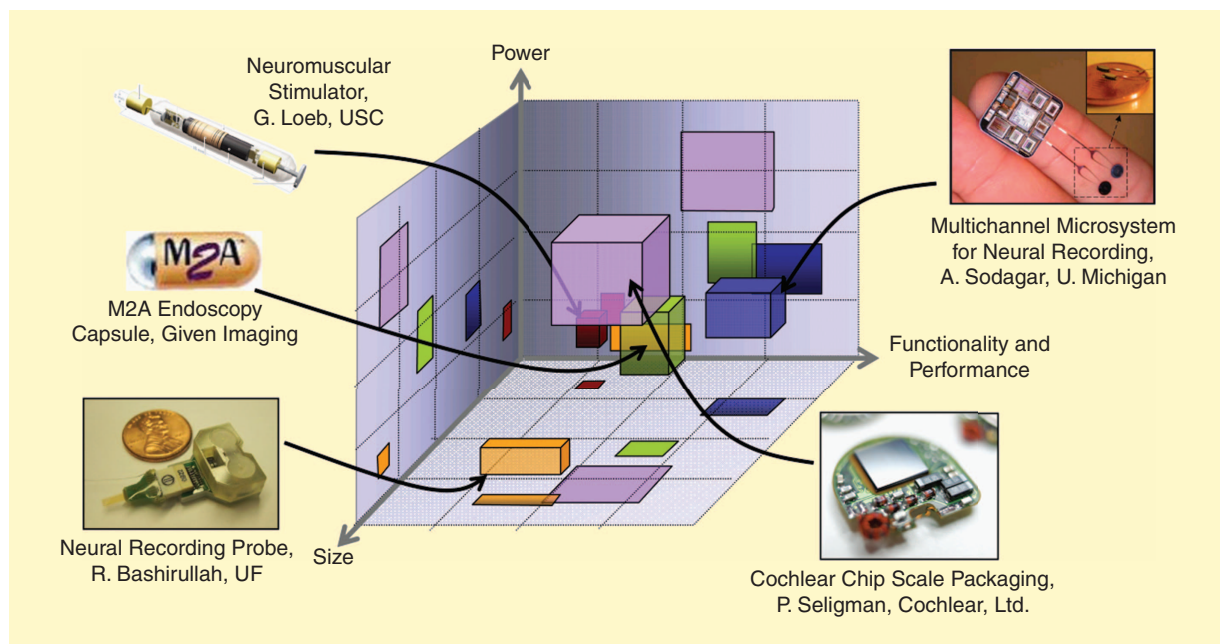


**Figure 1.** Parameterization of various biomedical hardware approaches in terms of size, power and functionality.

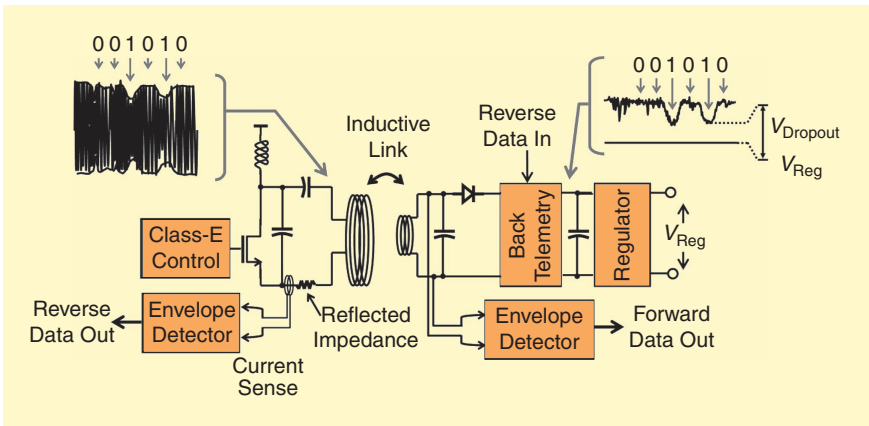


**Figure 2.** Basic inductive link components and architecture for wireless power and data transfer.

simple baseline approach for both power transfer and data telemetry. These implants can be made very small, highly integrated, and when necessary, entirely passive or without a battery. The power and data links can be separated both in frequency and space (that is, different antennas) to optimize each link independently, that is, high  $Q$  for power transfer and high bandwidth for data telemetry. Relatively simple direct conversion on/off keying (OOK) and amplitude shift keying (ASK) [9], [10] or frequency shift keying (FSK) [11], [12] transmitter topologies are often used for data transmission from the implant to the external unit, as shown in the simplified block diagram of Figure 3(a). Since the operating range is very short, the primary source of power dissipation is often the high-frequency modulator and local oscillator on-chip, which can eat up 50% or more of the total power budget allocated for the entire system [13]. One common technique to reduce power is to utilize a digitally programmable oscillator to tune and

drive an inductive antenna directly, thereby eliminating the power amplifier (PA) and buffers altogether [see Figure 3(b)]. Another approach circumvents the high-frequency local oscillator by replacing the active transmitter with a backscattering modulator [14]. RF backscatter modulators shift the burden of generating a higher-frequency carrier to the external detector or reader, thereby reducing the on-chip clock frequencies by one or two orders of magnitude [Figure 3(c)]. Receivers

for short-range links and moderate data rates of 10–100 kb/s also employ direct conversion ASK and/or FSK architectures based on simple envelope detectors and frequency discriminators, respectively. The dominant source of power dissipation typically stems from the desired receiver sensitivity instead of the clock and data recovery circuits that follow.

Longer-range telemetry links (>2 meters), such as those found in ingestible capsules, are predominantly battery operated and must conform to stricter regulatory standards. Longer range implies both higher sensitivity receivers and higher output power transmitters, both of which result in higher power dissipation. Moreover, unlike most short-range inductive links wherein a stable reference clock can be extracted from the external carrier frequency, battery operated devices often require stable crystal references and frequency synthesizers to generate a local carrier with high-frequency stability. These transceivers are typically operated in dedicated frequency bands such as the FCC approved 402–405 MHz for Medical Implant Communication Service (MICS) band. A case in point is the Zarlink RF transceiver [15] used in the wireless endoscopy capsule by Given Imaging (see the section “Ingestible Devices”). The transceiver consists of a 400-MHz low-IF superheterodyne architecture with image reject filters and FSK modulation scheme. An ultralow-power 2.45-GHz wake-up receiver with low duty cycle strobe is used to reduce the average current consumption, achieving standby currents of less than 250 nA. Thus, for longer-range battery-operated active transceivers, techniques such as duty cycling and wake-up receivers are essential to minimizing power. These systems should also operate at the highest possible data-rates, buffering data when necessary, to exploit duty-cycling of the power states to reduce the average current consumption [15]. Figure 4(a) and (b) shows the power dissipation versus data rate for recently published transmitters and receivers in the biomedical space. Although design choices are very application specific, there is an

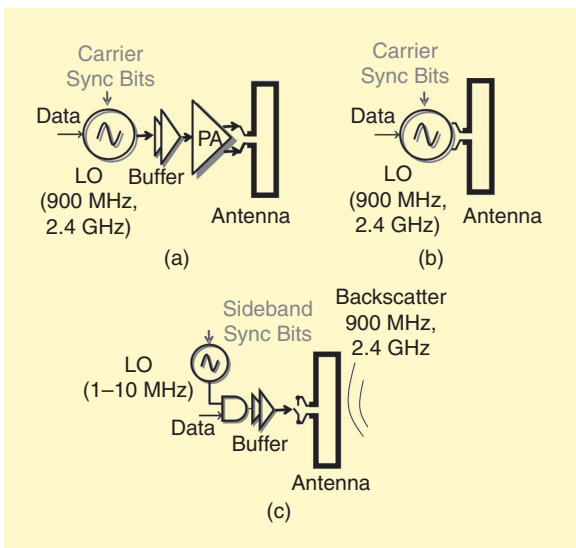


**Figure 3.** Simplified block diagrams of data transmission strategies for biomedical devices.

apparent correlation between desired bandwidth and power, as expected. Moreover, as shown in Figure 4(c), receivers with higher sensitivity dissipate more power and should be optimized accordingly for the desired communication range.

### Antenna and Frequency Considerations

Antennas for small-scale implants play an important role in determining the transmission loss and power budget of the RF link and thus the energy efficiency of the overall hardware platform [16]. Among the primary design considerations are in vivo losses due to tissue absorption, antenna size, and choice in operating frequency. For a critical review of the electrical properties of biological tissue in the body, see [17]. To illustrate the effect of tissue absorption as a function of frequency, normalized radiated near field contour plots generated by a small zig-zag dipole antenna placed inside the stomach are shown in Figure 5 for FCC approved 402–405 MHz for MICS, the 902–928 MHz, 2.4–2.483 GHz and 5.725–5.875 GHz industrial-scientific-medical (ISM) frequency bands [18]. A finite difference time domain (FDTD) tool from REMCOM Inc with a complete electrical model with 23 different tissue types of an average American male was used to determine the radiation characteristics [19]. In this example, the optimal radiation frequency lies near the 900 MHz band, as at lower frequencies the antenna is an inefficient radiator due to its size, and at higher frequencies tissue absorption losses dominate. Similar results are reported in [20]. Thus, while most biomedical links operate at much lower frequencies, the optimal choice of frequency depends on the size and type of antenna and its location in the body.

### Safety

Recommendations of safety levels with respect to human exposure to radio frequency electromagnetic fields are described in IEEE Standard C95.1-2005 [21]. These recommendations are expressed in terms of maximum permission exposures (MPEs) and specific absorption ratio (SAR) values. For instance, the SAR localized MPE is 2 W/kg averaged over six minutes. The SAR can be expressed in terms of  $SAR = \sigma E^2 / \rho$ , where  $\sigma$  is the tissue conductivity (S/m),  $\rho$  is the tissue density ( $\text{kg}/\text{m}^3$ ) and  $E$  is the root mean square (rms) electric field strength in tissue (V/m). For power transfer via inductive links, the resulting RF heating of the tissue is a primary safety concern. In general, tissue temperature rise must be kept to less than 1–2 °C to avoid cellular damage in sensitive areas such as the brain [22].

### Implantable Devices

#### Cardiac Pacemakers and Defibrillators

Advances in implantable pacemakers and defibrillators over the last half century have practically redefined

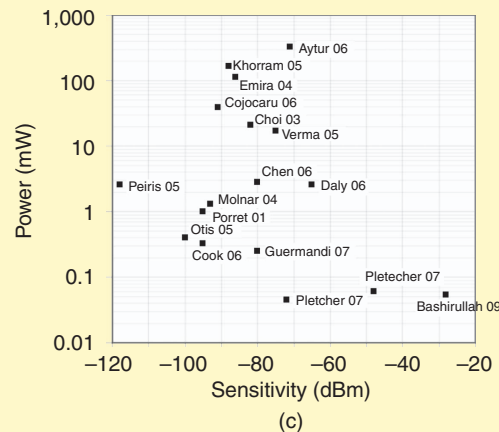
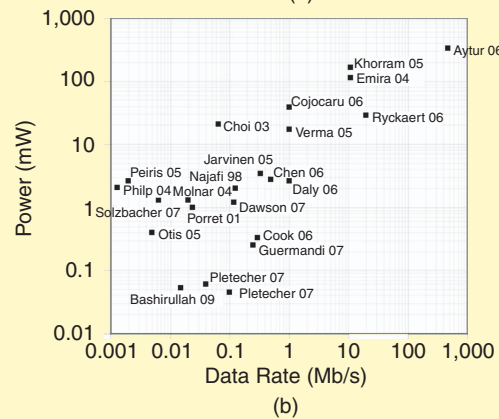
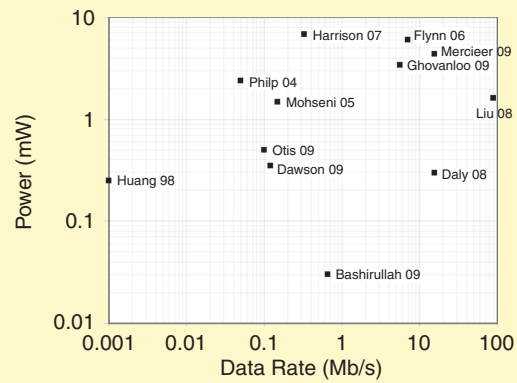


**Figure 4.** Published data of low-power communication links: (a) transmitter power versus data rate, (b) receiver power versus data rate, and (c) receiver power versus sensitivity.

life for patients suffering from heart disease. Since the introduction of the first pacemakers in the 1950s, the complexity of the implant system has increased from a mere few components and transistors to highly sophisticated medical devices with millions of transistors and extreme low-power operation to last 10–12 years from a single primary battery [23]–[25]. An example implantable pacemaker from St. Jude Medical is shown in Figure 6 [26]. The pacemaker consists of the pacing leads and the pacemaker device. The leads, made of flexible insulated wire with an electrode tip inserted

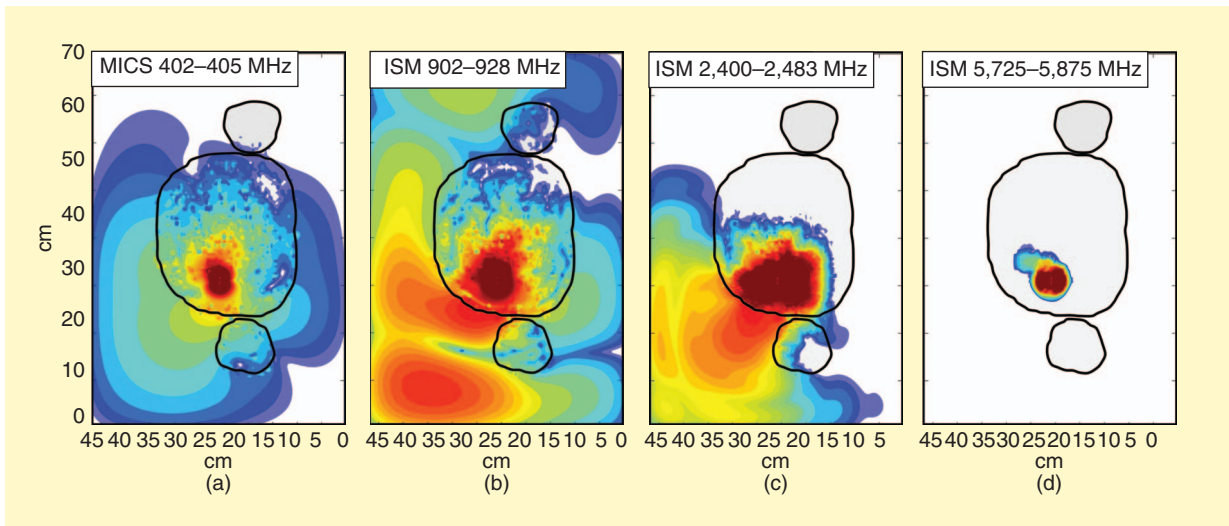


**Figure 5.** Cross section of human body model torso indicating the normalized radiation field intensity contours generated by a 14 mm by 3 mm zig-zag dipole antenna in the (a) MICS 402–405 MHz, (b) ISM 902–928 MHz, (c) ISM 2.4–2.483 GHz, and (d) ISM 5.725–5.875 GHz FCC frequency bands. Radiation is most efficient in the 902–928 MHz band. The smaller circles above and below the torso represent the arms of the subject.

through a vein into the heart, are used to stimulate the heart by carrying electrical impulses from the pacemaker device. As shown in Figure 6, the leads are also used to sense cardiac signals, which are subsequently amplified, filtered, and digitized to monitor the patient's heart rate and provide stimulation when required. The pacemaker integrated circuit (IC) is composed of a sensing system which consists of amplifiers, filters and analog-to-digital converter (ADC); a high-voltage multiplier and output stage for generating the stimulation pulses; a battery management system, wireless inductive link, and bias/reference generators; and signal processor that implement algorithms for therapy and timing control. As reported in [26], the 200 k transistor IC fabricated in a  $0.5\ \mu\text{m}$  3P-3M process occupies  $49\ \text{mm}^2$  and consumes only  $8\ \mu\text{W}$ ; deep sub-threshold designs and switched-capacitor techniques are widely used for low-power operation.

Unlike the implantable cardiac pacemakers used to treat pathological conditions known collectively as heart block, that is, cardiac arrhythmias such as bradycardia (slow heart rate), wherein the heart's natural pacemaking function is assisted using relatively low-voltage stimulation pulses (5–10 V) [27], implantable automatic defibrillators are able to deliver high-energy pulses of approximately 30–35 J at 750 V for  $\sim 4$ –8 ms in duration [23], [28]. The implantable defibrillator is a life support device that continuously monitors the patient's heart rhythm for abnormally fast heart rate, or tachycardia, and uncoordinated and disorganized heart rhythms known as cardiac fibrillation. When the device detects an abnormal heart rhythm, it shocks the heart into a normal rhythm with up to four to five pulses per event. The implantable defibrillator is similar but slightly

larger than the implantable pacemaker; it consists of a power supply (that is, battery), energy storage components and high-voltage devices for pulse generation, electrode leads for sensing and delivering stimulus pulses, a telemetry inductive link channel to program and individualize device behavior for each patient, and sensing/processing circuits for monitoring heart signals, collecting therapy history and diagnostic files, and monitoring all subsystem functions [28]. As in the case of the cardiac pacemaker, low current consumption (typically  $<10$ – $20\ \mu\text{A}$ ) in the implantable defibrillator is absolutely critical to meet the battery lifetime requirements.

### Visual Prosthesis

An emerging electronic biomedical implant aimed at restoring vision loss due to degeneration of the light sensing photoreceptors caused by incurable diseases such as retinitis pigmentosa (RP) and age-related macular degeneration (AMD) is reported in [29]. The prosthetic device is inspired by early discoveries that direct electrical stimulation of the retinal neurons creates visual sensation [30]. The overall system, as shown in Figure 7, consists of an external signal processing unit for complementary metal oxide semiconductor (CMOS) camera output, a bidirectional telemetry unit, an internal signal processing unit, a stimulus generator/driver, and an electrode array for interfacing to the retina [31], [32]. The communication link has two basic components—power and data transfer from the external to the internal unit, and data transfer from the internal to the external unit.

As in the case of most implants, an external class-E driver is used as the power coil transmitter owing to its high efficiency and ability to generate high field

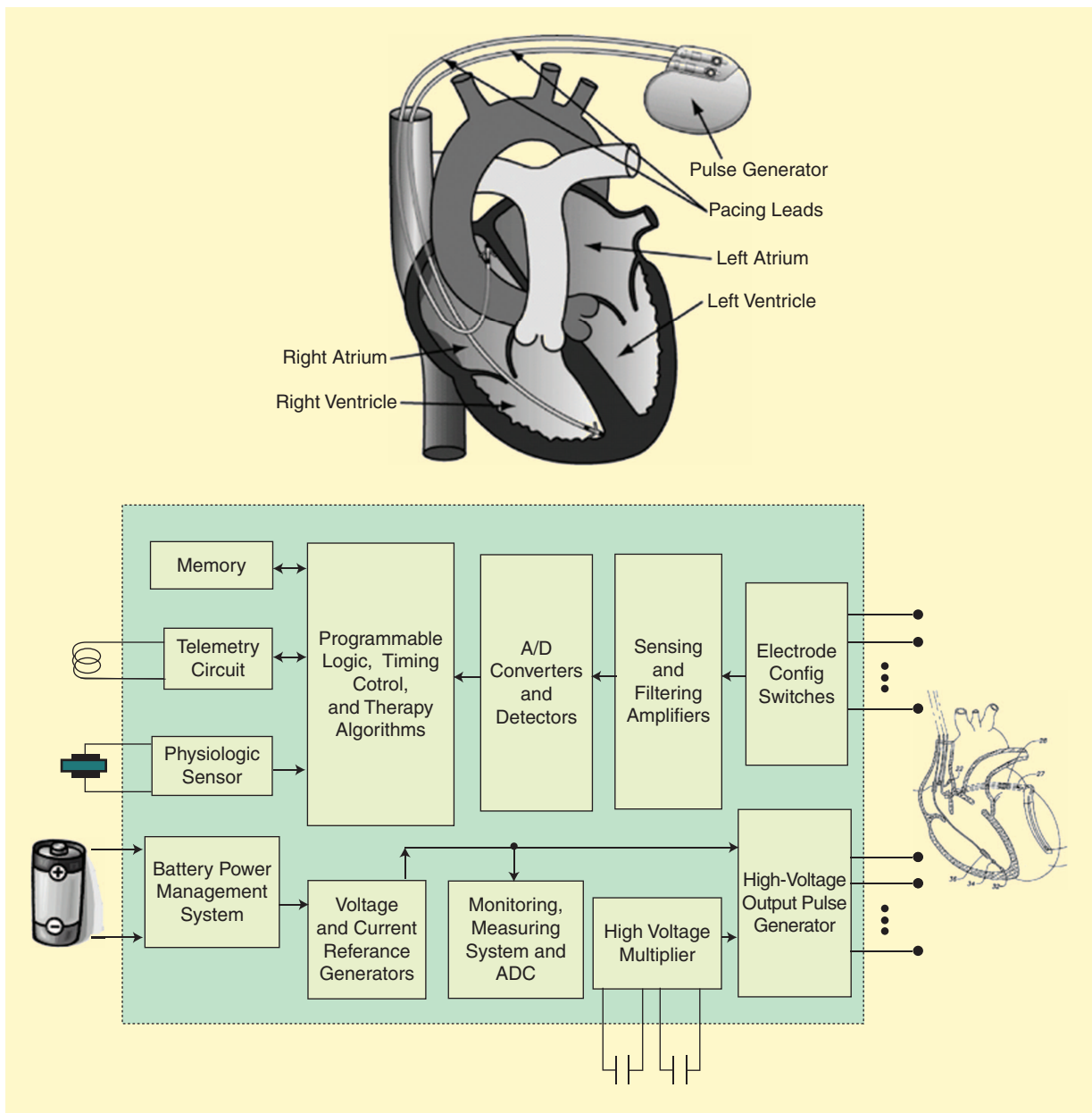


**Figure 6.** Cardiac pacemaker system [26].

strengths from a low-voltage power supply. The prototype system operates at 1 MHz to deliver up to 250 mW to the implant unit over a coil distance of 0.7 to 1.5 cm, corresponding to a coupling coefficient of 0.17 to 0.08 [31]. A back telemetry link sends digital data at 3.3 kbps from implant to external unit using the load modulation technique. The inductive power delivery system also features an adaptive controller to monitor coupling variations and changes in implant current loading to deliver power as required by the implant [33]. These variations can result in increased implant heating due to excess transmitted power, causing a detrimental effect on the tissue in the long term; or decreased implant supply voltage/current due to insufficient transmitted power, causing improper device operation or shutdown. Experi-

ments reported in [34] show that the closed-loop adaptive inductive link achieves a 2x improvement in efficiency—from 357 mW with adaptive control compared to 763 mW without.

### **Brain Computer Interfaces**

Neural interfaces convert brain signals into outputs that infer brain intentional states. As a communication channel it can be used to replace lost function such as voluntary arm or leg movement in patients with severe motor disabilities. Invasive signal recording methods for BCIs include electrocorticography (ECoG), electrical brain activity recorded beneath the cranium, and single-unit activity (SUA) recordings to monitor individual neuron action potential firing [35]. Although currently there is extensive research in both

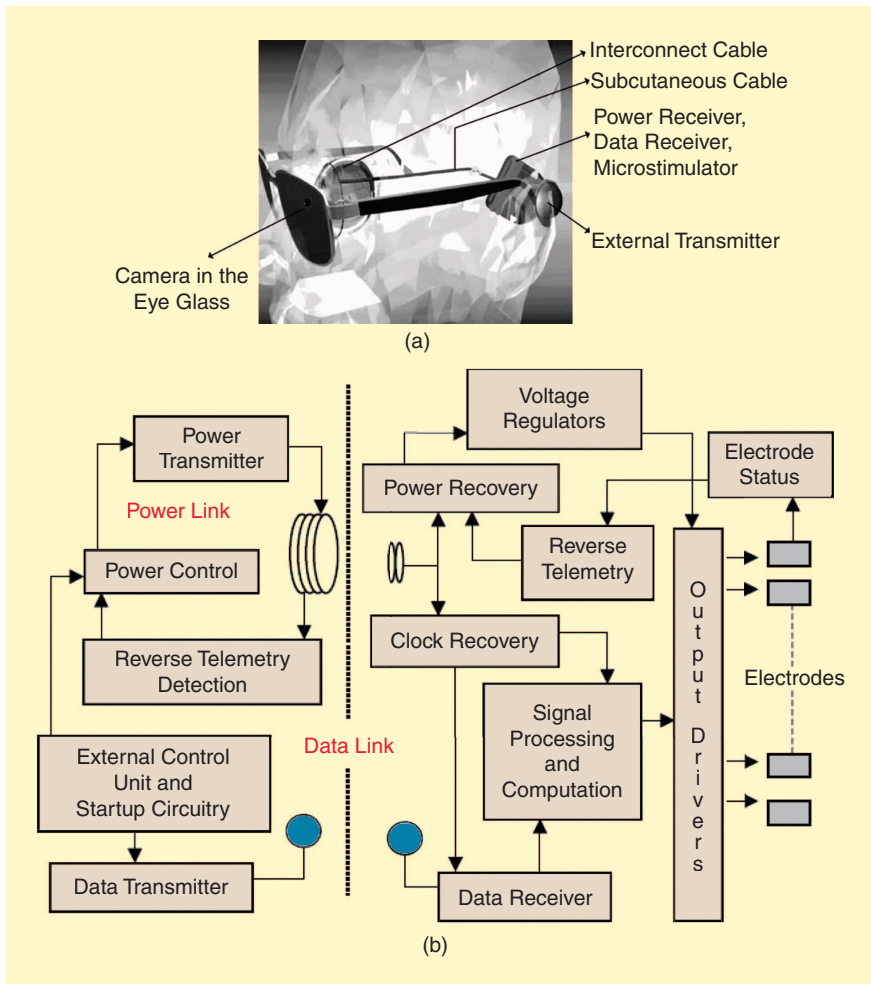


**Figure 7.** Visual prosthesis (a) conceptual diagram for epiretinal visual prosthesis and (b) simplified block of bidirectional telemetry unit [32].

modalities [35]–[38], several groups are implementing hardware approaches for direct neural interfaces based on SUA spike recordings as it provides high SNR, fine spatial resolution and localized action potentials for decoding very specific motor movements and/or cognitive tasks, with control signals of many degrees of freedom [39]–[46].

Hardware implementations for modular neural spike recording brain interfaces are presented in [22]. Lithographically defined probes in a standard silicon CMOS process in [22] have been used to interface up to 256 microelectrode recording sites with the amplifier and processing circuits fabricated in the same substrate as the electrodes. In [41], two 32-channel recording sites are interfaced to on-chip amplification and processing electronics using parylene ribbon interconnects, as shown in Figure 8(a). A 4–8 MHz inductive link is used for power and forward telemetry to transfer data toward the implant microsystem using phase-coherent FSK. The reverse telemetry link utilizes a dedicated OOK transmitter with its carrier frequency programmable from 70 to 200 MHz. Both links achieve reported data rates of 2 Mb/s for a channel scan rate of 62.5 kS/s

and overall system power dissipation is ~14.5 mW. Another approach reported in [42] utilizes the Utah Electrode Array (UEA), a 10 X 10 array of platinum-tipped silicon extracellular electrodes. As shown in Figure 8(b), the mixed-signal integrated circuit is flip-chip bonded to the back of the Utah Array to directly connect to all 100 electrodes. The complete system receives power and commands (at 6.5 kb/s) wirelessly over a 2.64 MHz inductive link and transmits neural data back at a data rate of 330 kb/s using a fully-integrated 433-MHz FSK transmitter with on-chip inductor. Power is also provided to the chip inductively via an off-chip 5-mm gold-on-polyimide coil [42]. The 4.7 by 5.9 mm<sup>2</sup> chip was fabricated in a 0.5 μm 3M-2P CMOS process and consumes 13.5 mW.

## Ingestible Devices

### Electronic Pill for Medication Compliance

Ingestible devices, unlike the chronically implanted devices, reside within the body only for a limited time to perform specific functions such as diagnosing of the gastrointestinal (GI) tract or reporting of useful medical observations (that is, core body temperature). An example application of new technology for ingestible devices is a medication adherence tag that consists of an electronic microchip and a biocompatible antenna inlay attached onto the surface of a standard 00-sized capsule with outer diameter of 8.53 mm and height or locked length of 23.30 mm, as shown in Figure 9(a) [47], [48]. Once this electronic pill (e-pill) is ingested, an external body worn reader establishes a communication link between the capsule transponder inside the GI tract and the reader. The e-pill transponder utilizes an electronic burst (eBurst) communication scheme to generate RF bursts larger than the incident power at any given time. The operation of the tagging system can be treated as a two-step energy conversion process. During the charging phase, a low frequency alternating signal from the external reader activates the tag to support nominal device functionality and establish the required charge on a storage capacitor to sustain a short RF burst during the discharge phase. In

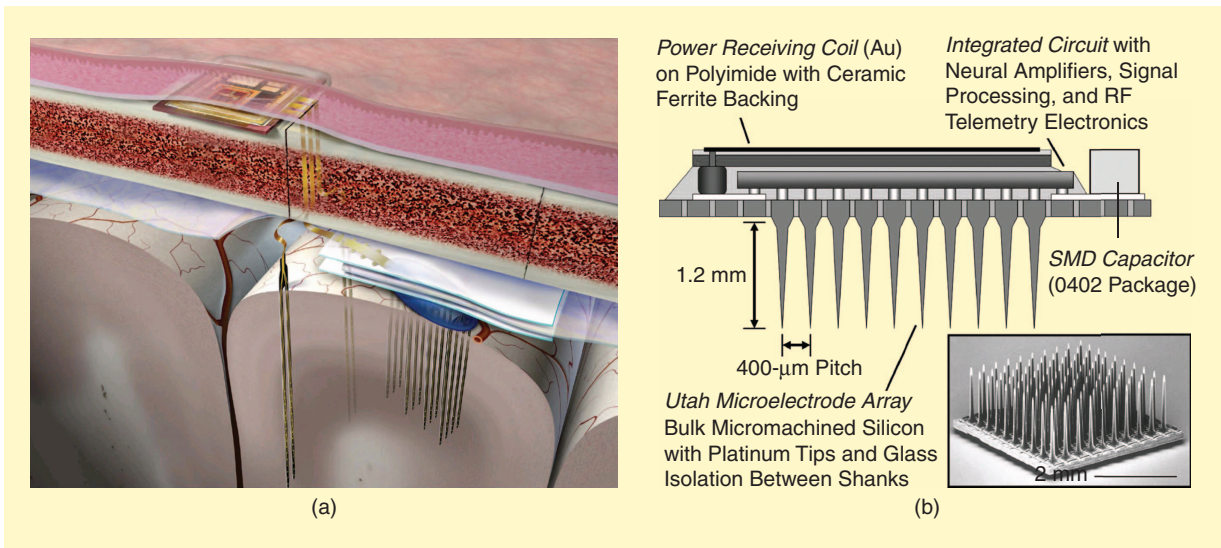


**Figure 8.** Conceptual diagrams of neural microsystems for brain computer interfaces: (a) two-dimensional and three-dimensional arrays of cortically implanted electrodes with ribbon cables connecting them to a subcutaneous electronics [41] and (b) neural interface (INI) assembly concept with Utah Microelectrode Array [42].

this phase, an active 915 MHz transmitter is enabled to generate a short RF burst until the storage capacitor is partially discharged, after which the tag re-enters the charging phase [48]. By detecting if and when the capsule is ingested, a patient's adherence to medications can be measured in terms of percent of doses taken over a period of time [49]. Another device developed by Proteus Biomedical, utilizes ingestible event markers (IEMs) that are tiny, digestible sensors powered by a food-like battery that is activated by stomach fluids after swallowing [50]. Once activated, the pills send signals to a receiver that is similar to a large bandage. The receiver records the date and time of the ingestion event. The IEM is the cornerstone of the company's Raisin System, which is currently under development.

### Video Capsule Endoscopy

Wireless capsule endoscopy, also known as video capsule endoscopy (VCE), is likely the most prominent ingestible in vivo electronic technology approved for clinical practice. Although it was only introduced in 2000, VCE has become the gold standard for endoscopic examination. The PillCam capsule, first introduced by Given Imaging [51], is small enough to be swallowable, typically measuring around 11 mm × 26 mm, and is battery powered. Images are captured as the capsule passes through the GI tract and transmitted wirelessly using an onboard RF transceiver that operates in the 402–405 MHz MICS band with a power output of –25 dBm. The technology has proven to be an effective modality in diagnosing many small bowel diseases such as obscure GI bleeding, Crohn's disease, GI polyposis syndromes, and small bowel tumors. The PillCam capsule [shown in Figure 9(b)] includes an optical dome with a lens holder and a short focal length lens, four

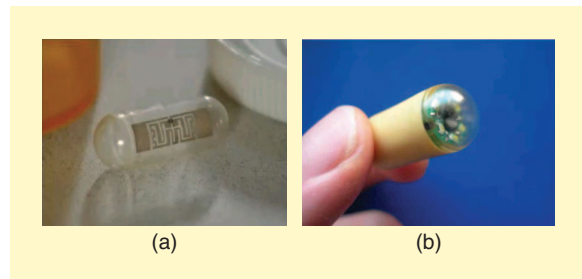


**Figure 9.** Ingestible capsules: (a) an electronic pill for medication adherence monitoring [48] (reprinted with permission), and (b) Given Imaging M2A endoscopic capsule [53].

light emitting diodes (LEDs), a CMOS image sensor, two silver oxide batteries, and an ASIC RF transmitter with an external receiving antenna [52]. The PillCam transmits up to 14 images/s, or 2,600 images assuming the capsule remains ~8 hrs in the small intestine and 15–20 minutes in the esophagus. A critical challenge for this technology is to image the entire GI tract within the capacity limits of the on-board batteries.

### Conclusions

In vivo wireless biomedical devices hold the promise to become one of the major technology drivers of the 21st century. With continued advances in electronic component integration, sensor development, and micropackaging technologies, these biomedical devices will achieve widespread use in a myriad of emerging biomedical applications aimed at improving quality of life.

This article presented a brief overview of design considerations for implementing wireless power and data interfaces for in vivo biomedical devices. The basic hardware challenges stems from tradeoffs in



## 2011 IEEE Topical Meeting on Biomedical Radio and Wireless Technologies, Networks, and Sensing Systems

The IEEE Topical Conference on Biomedical Wireless Technologies, Networks, and Sensing Systems (BioWireleSS) will premier in sunny Phoenix, Arizona, at the Renaissance Glendale Hotel 16–20 January. This two-day topical conference will be a vital part of the IEEE Radio and Wireless Symposium, featuring the latest developments in wireless biomedical technologies, networks, and sensing systems.

The wireless revolution has begun to infiltrate the medical community with patient health monitoring, telesurgery, mobile wireless biosensor systems, and wireless tracking of patients and assets becoming a reality. The rapid evolution of wireless technologies coupled with powerful advances in adjacent fields such as biosensor design, low-power battery operated systems, and diagnosing and reporting for intelligent information management has opened up a plethora of new applications for wireless systems in medicine. Papers featuring innovative work will be presented in the following areas of biomedical wireless technologies, networks, and sensing systems:

- wireless technologies for micromedical sensors
- wireless positioning technologies in medicine
- microwave imaging for biomedical applications
- personal area networks and body area networks

- advanced wireless digital systems including Energy Scavenging for Health Monitoring
- microwave systems for biological applications
- microwave interaction with biological tissues
- coexistence and modeling of wireless technologies in medical environments
- biomedical devices for remote patient monitoring
- high data rate protocols and processing for biosignals
- microwave systems for therapeutic biomedical applications

The conference will provide a healthy mix of actual clinical work incorporating wireless technologies with more fundamental science and engineering research in this area. Sessions will feature world-renowned invited speakers in their respective research areas, covering a wide range of topics related to all aspects of the conference. We are excited about this emerging area of research and look forward to the coming together of medical professionals, engineers, and industry representatives.

We also hope you take advantage of the sunshine and warmer temperatures in Phoenix by playing a round of golf, checking out the local boutiques, or even taking a day hike.

We look forward to seeing you in sunny Arizona!

—Mohamed R. Mahfouz and Rizwan Bashirullah  
Co-chairs IEEE BioWireleSS 2011

Digital Object Identifier 10.1109/MMM.2010.938580

implant size, power dissipation and system functionality. Wireless powering of biomedical implants is primarily via low frequency inductively coupled links as at low frequencies the RF heating due to tissue absorption is minimized. And while data telemetry between extracorporeal and in vivo devices is typically implemented by modulating the amplitude or frequency of the power carrier and/or changing the load impedance of secondary coil, highly power efficient communication links are feasible by optimizing and separating the power and data links. For optimum data link performance, the choice of operating frequency and antenna design becomes critical. These basic design considerations have been shown in the context of in vivo biomedical systems such as implantable visual and neural interfaces and ingestible capsule technologies.

### Acknowledgments

This work has been partially supported by grants from the National Institute of Health (NIH/NINDS-R01 NS053561-01A2), the National Science Foundation (NSF) via the Career Award (NSF-0547057), Convergent Engineering via SBIR support from the

NSF, and matching funds from the Florida High Tech Corridor Council (FHTCC) at the University of Florida.

### References

- [1] W. H. Ko, S. P. Liang, and C. D. Fung, "Design of radio-frequency powered coils for implant instruments," *Med. Biol. Eng. Comput.*, vol. 15, no. 6 pp. 634–640, Nov. 1977.
- [2] K. Finkenzerler, *RFID Handbook: Fundamental and Applications in Contactless Smart Cards and Identification*, 2nd ed. West Sussex, U.K.: Wiley, 2003.
- [3] K. R. Foster and H. P. Schwan, "Dielectric properties of tissues and biological materials: A critical review," *CRC Crit. Rev. Bio. Eng.*, vol. 17, no. 1, pp. 25–104, 1989.
- [4] D. G. Galbraith, M. Soma, and R. L. White, "A wide-band efficient inductive transdermal power and data link with coupling insensitive gain," *IEEE Trans. Biomed. Eng.*, vol. 34, pp. 265–275, Apr. 1987.
- [5] C. Zierhofer and E. Hochmair, "Geometric approach for coupling enhancement of magnetically coupled coils," *IEEE Trans. Biomed. Eng.*, vol. 43, no. 7, pp. 708–714, July 1996.
- [6] N. Sokal and A. D. Sokal, "A class-E: A new class of high-efficiency tuned single-ended switching power amplifier," *IEEE J. Solid State Circuits*, vol. 10, no. 3, pp. 168–176, June 1975.
- [7] Z. Tang, B. Smith, J. H. Schild, and P. H. Peckham, "Data transmission from an implantable biotelemeter by load-shift keying using circuit configuration modulator," *IEEE Trans. Biomed. Eng.*, vol. 42, no. 5, pp. 524–528, May 1995.

- [8] W. Liu, P. Singh, C. DeMarco, R. Bashirullah, M. S. Humayun, and J. D. Weiland, *Semiconductor-Based Implantable Microsystems*. Boca Raton, FL: CRC, 2003.
- [9] P. R. Troyk and M. A. K. Schwan, "Closed-loop class E transcutaneous power and data link for microimplants," *IEEE Trans. Biomed. Eng.*, vol. 39, no. 6, pp. 589–599, June 1992.
- [10] T. Akin, K. Najafi, and R. M. Bradley, "A wireless implantable multichannel digital neural recording system for a micromachined sieve electrode," *IEEE J. Solid-State Circuits*, vol. 33, no. 1, pp. 109–118, Jan. 1998.
- [11] M. Ghovanloo and K. Najafi, "A wide-band frequency-shift keying wireless link for inductively powered biomedical implants," *IEEE Trans. Circuits Syst. I*, vol. 51, no. 12, pp. 2374–2383, Dec. 2004.
- [12] P. Mohseni and K. Najafi, "Wireless multi-channel biopotential recording using an integrated FM telemetry circuit," *IEEE Trans. Neural. Syst. Rehabil. Eng.*, vol. 13, pp. 263–271, Sept. 2005.
- [13] H. Yu, P. Li, Z. Xiao, C.-C. Peng, and R. Bashirullah, "A multichannel instrumentation system for biosignal recording," in *Proc. IEEE Int. Conf. Engineering in Medicine and Biology Society (EMBS)*, Aug. 20, 2008, pp. 2020–2023.
- [14] Z. Xiao, C.-M. Tang, C.-C. Peng, H. Yu, and R. Bashirullah, "A 190uW-915MHz active neural transponder with 4-channel time multiplexed AFE," in *Proc. IEEE VLSI Circuits Symp.*, June 2009, pp. 58–59.
- [15] P. D. Bradley, "An ultra low power, high performance medical implant communication system (MICS) transceiver for implantable devices," in *Proc. IEEE BioCas*, Nov. 2006, pp. 158–161.
- [16] H. A. Wheeler, "Fundamental limitations of small antennas," *Proc. IRE*, vol. 35, no. 12, pp. 1479–1488, Dec. 1947.
- [17] S. Gabriel, R. W. Lau, and C. Gabriel, "The dielectric properties of biological tissues: II. Measurements in the frequency range 10 Hz to 20 GHz," *Phys. Med. Biol.*, vol. 41, no. 11, pp. 2251–2269, Nov. 1996.
- [18] H. Yu, G. S. Irby, D. M. Peterson, M.-T. Nguyen, G. Flores, N. Euliano, and R. Bashirullah, "Printed capsule antenna for medication compliance monitoring," *Electron. Lett.*, vol. 43, no. 22, pp. 1179–1181, Oct. 2007.
- [19] REMCOM, Inc [Online]. Available: [www.remcom.com](http://www.remcom.com)
- [20] L. C. Chirwa, P. A. Hammond, S. Roy, and D. R. S. Cumming, "Electromagnetic radiation from ingested sources in the human intestine between 150 MHz and 1.2 GHz," *IEEE Trans. Biomed. Eng.*, vol. 50, no. 4, pp. 484–492, Apr. 2003.
- [21] *IEEE Standard for Safety Levels with Respect to Human Exposure to Radio Frequency Electromagnetic Fields, 3 kHz to 300 GHz*, IEEE C95.1-2005, 2006.
- [22] K. D. Wise, A. M. Sodagar, Y. Yao, M. N. Gulari, G. E. Perlin, and K. Najafi, "Microelectrodes, microelectronics, and implantable neural microsystems," *Proc. IEEE*, vol. 96, no. 7, pp. 1184–1202, July 2008.
- [23] J. G. Webster, *Medical Instrumentation Application and Design*, 4th ed. New York: Wiley, 2010.
- [24] Medtronic [Online]. Available: [www.medtronic.com](http://www.medtronic.com)
- [25] Boston Scientific [Online]. Available: [www.bostonscientific.com](http://www.bostonscientific.com)
- [26] L. S. Y. Wong, S. Hossain, A. Ta, J. Edvinsson, D. H. Rivas, and H. Nääs, "A very low-power CMOS mixed-signal IC for implantable pacemaker applications," *IEEE J. Solid-State Circuits*, vol. 39, no. 12, pp. 2446–2456, Dec. 2004.
- [27] J. Ryan, K. Carroll, and B. Pless, "A four chip implantable defibrillator/pacemaker chipset," in *Proc. IEEE Custom Integrated Circuit Conf.*, May 1989, pp. 7.6.1–7.6.4.
- [28] J. A. Warren, R. D. Dreher, R. V. Jaworski, J. Putzke, and R. J. Russie, "Implantable cardioverter defibrillators," *Proc. IEEE*, vol. 84, no. 3, pp. 468–479, Mar. 1996.
- [29] M. Humayun, E. de Juan, Jr., J. D. Weiland, G. Dagnelie, and G. D. Katona, "Pattern electrical stimulation of the human retina," *Vision Res.*, vol. 39, no. 15, pp. 2569–2576, July 1999.
- [30] G. Brindley and W. Lewin, "The sensations produced by electrical stimulation of the visual cortex," *J. Physiol. (London)*, vol. 196, no. 2, pp. 479–493, May 1968.
- [31] W. Liu, M. Sivaprakasam, P. R. Singh, R. Bashirullah, and G. Wang, "Electronic visual prostheses," *Artif. Organs*, vol. 27, no. 11, pp. 986–995, Nov. 2003.
- [32] M. Sivaprakasam, W. Liu, G. Wang, J. D. Weiland, and M. S. Humayun, "Architecture tradeoffs in high-density microstimulators for retinal prosthesis," *IEEE Trans. Circuits Syst. I*, vol. 52, no. 12, pp. 2629–2641, Dec. 2005.
- [33] R. Bashirullah, W. Liu, Y. Ji, A. Kendir, M. Sivaprakasam, G. Wang, and B. Pundi, "A smart bi-directional telemetry unit for retinal prosthetic device," in *IEEE Proc. Int. Symp. Circuits and Systems*, May 25–28, 2003, vol. 5, pp. 5–8.
- [34] G. Wang, W. Liu, M. Sivaprakasam, and G. A. Kendir, "Design and analysis of an adaptive transcutaneous power telemetry for biomedical implants," *IEEE Trans. Circuits Syst. I*, vol. 52, no. 10, pp. 2109–2117, Oct. 2005.
- [35] M. Nicoletti, "Actions from thoughts," *Nature*, vol. 409, no. 6818, pp. 403–407, 2001.
- [36] J. P. Donoghue, "Connecting cortex to machines: Recent advances in brain interfaces," *Nat. Neurosci.*, vol. 5, pp. 1085–1088, Oct. 2002.
- [37] J. R. Wolpaw, N. Birbaumer, D. J. McFarland, G. Pfurtscheller, and T. M. Vaughan, "Brain-computer interfaces for communication and control," *Clin. Neurophysiol.*, vol. 113, no. 6, pp. 767–791, June 2002.
- [38] E. C. Leuthardt, G. Schalk, J. W. Wolpaw, J. G. Ojemann, and D. W. Moran, "A brain computer interface using electrocorticographic signals in humans," *J. Neural Eng.*, vol. 1, no. 2, pp. 63–71, June 2004.
- [39] R. Bashirullah, J. Harris, J. Sanchez, T. Nishida, and J. Principe, "Florida wireless implantable recording electrodes (FWIRE) for brain machine interfaces," in *Proc. IEEE Int. Symp. Circuits and Systems*, New Orleans, LA, May 2007, pp. 2084–2087.
- [40] J. C. Sanchez, J. C. Principe, T. Nishida, R. Bashirullah, J. G. Harris, and J. Fortes, "Technology and signal processing for brain-machine interfaces," *IEEE Signal Processing Mag.*, vol. 25, no. 1, pp. 29–40, Dec. 2008.
- [41] A. M. Sodagar, K. D. Wise, and K. Najafi, "A wireless implantable microsystem for multichannel neural recording," *IEEE Trans. Microwave Theory Tech.*, vol. 57, no. 10, pp. 2565–2573, Oct. 2009.
- [42] R. R. Harrison, P. T. Watkins, R. J. Kier, R. O. Lovejoy, D. J. Black, B. Greger, and F. Solzbacher, "A low-power integrated circuit for a wireless 100-electrode neural recording system," *IEEE J. Solid-State Circuits*, vol. 42, no. 1, pp. 123–133, Jan. 2007.
- [43] A. Avestruz, W. Santa, D. Carlson, R. Jensen, S. Stanslaski, A. Helfenstine, and T. Denison, "A 5 uW/channel spectral analysis IC for chronic bidirectional brain-machine interfaces," *IEEE J. Solid-State Circuits*, vol. 43, no. 12, pp. 3006–3024, Dec. 2008.
- [44] R. Sarpeshkar, W. Wattanapanitch, B. I. Rapoport, S. K. Arfin, M. W. Baker, S. Mandal, M. S. Fee, S. Musallam, and R. A. Andersen, "Low-power circuits for brain-machine interfaces," in *Proc. 2007 IEEE Int. Symp. Circuits Syst.*, May 2007, pp. 2068–2071.
- [45] J. Lee, H.-G. Rhew, D. Kipke, and M. Flynn, "A 64 channel programmable closed-loop deep brain stimulator with 8 channel neural amplifier and logarithmic ADC," in *Symp. VLSI Circuits Dig.*, June 2008, pp. 76–77.
- [46] S. Farshchi, D. Markovic, S. Pamarti, B. Razavi, and J. W. Judy, "Towards neuromote: A single-chip, 100-channel, neural-signal acquisition, processing, and telemetry device," in *Proc. 29th Annu. Int. Conf. IEEE Engineering in Medicine and Biology Society*, Aug. 23–26, 2007, pp. 437–440.
- [47] H. Yu, C.-M. Tang, and R. Bashirullah, "An asymmetric RF tagging IC for ingestible medication compliance capsules," in *Proc. IEEE Radio Frequency Integrated Circuits (RFIC) Symp.*, June 2009, pp. 101–104.
- [48] A. Hoover and K. Howell, "Rx for health: Engineers design pill that signals it has been swallowed," *University of Florida News*, Mar. 31, 2010.
- [49] K. C. Farmer, "Methods for measuring and monitoring medication regimen adherence in clinical trials and clinical practice," *Clin. Ther.*, vol. 21, no. 6, pp. 1074–1090, June 1999.
- [50] Proteus Biomedical [Online]. Available: [www.proteusbiomed.com](http://www.proteusbiomed.com)
- [51] G. Meron, "The development of the swallowable video capsule (M2A)," *Gastrointest. Endosc.*, vol. 52, no. 6, pp. 817–819, Dec. 2000.
- [52] A. Moglia, A. Mencias, and P. Dario, "Recent patents on wireless capsule endoscopy," *Recent Pat. Biomed. Eng.*, vol. 1, no. 1, pp. 24–33, Jan. 2008.
- [53] F. Carpi, S. Galbiati, and A. Carpi, "Controlled navigation of endoscopic capsules: Concept and preliminary experimental investigations," *IEEE Trans. Biomed. Eng.*, vol. 54, no. 11, pp. 2028–2036, Nov. 2007. 